2010

MOF and histone H4 acetylation at lysine 16 are critical for DNA damage response and double-strand break repair

Girdhar G. Sharma
Washington University School of Medicine in St. Louis

Sairei So
University of Texas Southwestern Medical Center at Dallas

Arun Gupta
Washington University School of Medicine in St. Louis

Rakesh Kumar
Washington University School of Medicine in St. Louis

Christelle Cayrou
Laval University

See next page for additional authors

Molecular and Cellular Biology

MOF and Histone H4 Acetylation at Lysine 16 Are Critical for DNA Damage Response and Double-Strand Break Repair

Girdhar G. Sharma, Sairei So, Arun Gupta, Rakesh Kumar, Christelle Cayrou, Nikita Avvakumov, Utpal Bhadra, Raj K. Pandita, Matthew H. Porteus, David J. Chen, Jacques Cote and Tej K. Pandita

Mol. Cell. Biol. **2010, 30(14):3582. DOI: 10.1128/MCB.01476-09.**
Published Ahead of Print 17 May 2010.

MOLECULAR AND CELLULAR BIOLOGY, July 2010, p. 3582–3595 Vol. 30, No. 14
0270-7306/10/$12.00 doi:10.1128/MCB.01476-09

MOF and Histone H4 Acetylation at Lysine 16 Are Critical for DNA Damage Response and Double-Strand Break Repair▽†

Girdhar G. Sharma,[1]§ Sairei So,[2]§ Arun Gupta,[1,2]§ Rakesh Kumar,[1,2]§ Christelle Cayrou,[3]‡ Nikita Avvakumov,[3] Utpal Bhadra,[4] Raj K. Pandita,[1] Matthew H. Porteus,[2] David J. Chen,[2] Jacques Cote,[3] and Tej K. Pandita[1,2]*

Washington University School of Medicine, St. Louis, Missouri 63108[1]; University of Texas, Southwestern Medical Center, Dallas, Texas 75390[2]; Laval University Cancer Research Center, Quebec City G1R 2J6, Canada[3]; and Centre for Cellular and Molecular Biology, Hyderabad AP 500007, India[4]

Received 11 November 2009/Returned for modification 21 January 2010/Accepted 4 May 2010

The human *MOF* gene encodes a protein that specifically acetylates histone H4 at lysine 16 (H4K16ac). Here we show that reduced levels of H4K16ac correlate with a defective DNA damage response (DDR) and double-strand break (DSB) repair to ionizing radiation (IR). The defect, however, is not due to altered expression of proteins involved in DDR. Abrogation of IR-induced DDR by MOF depletion is inhibited by blocking H4K16ac deacetylation. MOF was found to be associated with the DNA-dependent protein kinase catalytic subunit (DNA-PKcs), a protein involved in nonhomologous end-joining (NHEJ) repair. ATM-dependent IR-induced phosphorylation of DNA-PKcs was also abrogated in MOF-depleted cells. Our data indicate that MOF depletion greatly decreased DNA double-strand break repair by both NHEJ and homologous recombination (HR). In addition, MOF activity was associated with general chromatin upon DNA damage and colocalized with the synaptonemal complex in male meiocytes. We propose that MOF, through H4K16ac (histone code), has a critical role at multiple stages in the cellular DNA damage response and DSB repair.

In eukaryotes, specifically in mammals, the mechanisms by which the DNA damage response (DDR) components gain access to broken DNA in compacted chromatin remain a mystery. The DNA damage response occurs within the context of chromatin, and its structure is altered post-DNA double-strand break (DSB) induction. Major alterations include (i) chromatin remodeling via ATP-dependent activities and covalent histone modifications and (ii) incorporation of histone variants into nucleosomes. Chromatin structure creates a natural barrier to damaged DNA sites, which suggests that histone modifications will play a primary role in DDR by facilitating repair protein access to DNA breaks (43, 58, 87, 88). While some experimental evidence indicates that preexisting histone modifications may play an important role in DDR, the precise role of chromatin status prior to DNA damage on DDR is yet to be clearly established. For instance, biochemical and cell biology studies indicate that repair proteins (53BP1, *Schizosaccharomyces pombe* Crb2 [SpCrb2], and *Saccharomyces cerevisiae* Rad9 [ScRad9]) require methylated Lys79 of histone H3 (H3-K79) (29) or methylated Lys20 of histone H4 (H4-K20) and/or CBP/p300-mediated acetylation of histone H3 on lysine 56 (9, 15, 29, 66, 93) for focus formation at DNA-damaged sites. These modifications are normally present on chromatin, and none has been reported to change in response to ionizing radiation (IR)-induced DNA damage. However, it is yet to be established whether preexisting acetylation of specific histone residues at the time of cellular exposure to IR plays any critical role in DDR. While recent studies demonstrate that in human cells, histone H3 acetylated at K9 (H3K9ac) and H3K56ac are rapidly and reversibly reduced in response to DNA damage, most histone acetylation modifications do not change appreciably after genotoxic stress (80).

The amino-terminal tail of histone H4 is a well-described target for posttranslational modification, including acetylation (4, 19, 82). Reversible acetylation occurs at four lysines (positions 5, 8, 12, and 16) *in vivo* in most eukaryotes (4), and their hyperacetylation could lead to unfolding of the nucleosomal fiber (82). Acetylation of K16 is prevalent in *Drosophila* on the hyperactive male *Drosophila* polytene X chromosomes (83), where it contributes to transcriptional upregulation (22). In yeast, H4K16ac does not correlate with active genes (37), while all other known acetylation marks on histone H4 are linked to enhanced transcription (16). The H4K16ac modification poses a structural constraint on formation of higher-order chromatin. It is therefore possible that this posttranslational modification could contribute to DDR by forcing chromatin to keep a more open configuration. In this role, H4K16ac would potentially serve as a platform structure to generate proper signaling for DDR.

The histone acetyltransferase (HAT) responsible for the majority of H4K16 acetylation in the cell is MOF (2, 24, 25, 46, 75, 79). A single histone H4K16ac modification modulates both higher-order chromatin structure and functional interactions between a nonhistone protein and the chromatin fiber (74). The yeast histone acetyletransferase Esa1 (essential SAS2-related acetyltransferase), can acetylate lysine 16 of histone H4

* Corresponding author. Mailing address: Department of Radiation Oncology, UT Southwestern Medical Center, 2201 Inwood Road, NC7.116, Dallas, TX 75390. Phone: (214) 648-1918. Fax: (214) 648-5995. E-mail: tej.pandita@utsouthwestern.edu.

‡ Present address: Institute of Human Genetics, Montpellier, France.

§ These authors contributed equally.

† Supplemental material for this article may be found at http://mcb.asm.org/.

▽ Published ahead of print on 17 May 2010.

and is required for DNA repair in yeast (8). We have previously reported that cells expressing a HAT-dead human MOF (hMOF) had a higher frequency of residual DNA DSBs and chromosome aberrations after cellular exposure to IR; however, the reasons for the increased aberrations are not known (25). While histone lysine modifications have been linked to the recruitment of DNA repair factor in mammalian cells, it is unknown whether reduction of H4K16ac will influence DDR. Here we demonstrate that decreased levels of H4K16ac, due to hMOF depletion, can alter DDR at several stages of DNA DSB repair and abrogate both the non-homologous end-joining (NHEJ) and homologous recombination (HR) pathways of DNA repair.

MATERIALS AND METHODS

Cell culture and derivation of cell lines. HEK293, MCF7, HCT116, GM5849, and HL60 cells were maintained and transfected with plasmids as described previously (25). A cDNA fragment encoding wild-type hMOF was cloned into the mammalian expression vector pcDNA3.1 (Invitrogen, Carlsbad, CA) as described previously (24, 25). Wild-type hMOF was created by using a PCR approach with appropriate primer pair combinations.

RNAi. Small interfering RNAs (siRNAs) for MOF, Tip60, and control luciferase (Luc) were obtained from Dharmacon Research (Lafayette, CO). siRNA was labeled with Cy3 by using the Label IT siRNA Tracker intracellular localization kit (Mirus) following the manufacturer's prescribed procedure. RNA interference (RNAi) treatment of 293 and MCF7 cells, as well as cells from other cell lines, was performed as described previously (25, 26, 54). Cells were used 72 h after transfection for all experimental purposes. In some of our experiments, the siRNA sequence of CUCCCAGCCUGUAAAUAUGUU specific for the untranscribed region (UTR) of hMOF from Dharmacon was used to knock down endogenous hMOF.

Expression profiling. We have used the previously described modified approach for microarray analysis of gene expression (85). Total RNA was isolated from cells using the RNeasy kit (Qiagen, Inc., Valencia, CA), and expression analyses were performed using Affymetrix's commercial gene expression arrays. All experiments were performed at least in triplicate using enhanced green fluorescent protein (EGPF) double-stranded RNA (dsRNA)-treated samples as a control. We processed Raw Affymetrix CEL files by using MAS5.0 (92), and the nonspecific filtering was applied to probe sets having interquantile range values below 0.5. The remaining processed $\log_2$ intensity values were analyzed using the Bioconductor limma package (23) to detect differential gene expression. Statistical significance of the results was determined using a moderated eBayes *t* test. The resulting *P* values were adjusted using FDR (34). Probe sets were mapped to genes using the annotation available in Ensembl (21).

Western blot analysis, IP, ChIP, and complex purification. Cell lysates for Western blot analysis were prepared as previously described (54). Antibodies for the different proteins analyzed have been described previously (24–26). Immunoblotting and detection of hMOF, H4K16 acetylation, Tip60, and the DNA-dependent protein kinase catalytic subunit (DNA-PKcs) were done according to a previously described procedure (24, 25). For immunoprecipitation (IP), cells were broken in lysis buffer as described previously (25). Lysates were precleared with purified immunoglobulin G (IgG) and protein A/G beads. Proteins were immunoprecipitated with specific antibodies, and immunoprecipitates were washed with lysis buffer as described previously (25). For chromatin immunoprecipitation (ChIP), nuclear extracts were prepared as follows: 5×10^8 cells were pelleted, washed in phosphate-buffered saline (PBS), swollen in hypotonic buffer on ice (20 mM HEPES, pH 7.2, 0.3 M sucrose, 3 mM $MgCl_2$, 3 mM β-mercaptoethanol, 0.5 mM phenylmethylsulfonyl fluoride), and homogenized with 20 strokes of a loose-fitting Dounce pestle. Cellular homogenates were layered on a 0.65 M sucrose cushion and pelleted at $1,000 \times g$ for 5 min, and nuclei were resuspended in DNase I buffer and digested by the procedure previously described (47). Nuclear extracts in DNase I buffer were added to protein A-agarose beads that were prebound with antibody. Immunoprecipitates were washed with a buffer composed of 20 mM HEPES, pH 7.2, 10% glycerol, 0.35 M NaCl, 1 mM $MgCl_2$, and 0.5 mM phenylmethylsulfonyl fluoride. For tandem affinity purification (TAP) of native complexes with nuclear extracts, fractionation on immunoglobulin G (IgG)-Sepharose and calmodulin resin was performed as described previously (18). For the identification of the stable components of purified complexes, we performed silver staining, tandem mass spectrometry, and Western blotting as previously described (75). Chromatin immunoprecipitation after formaldehyde-mediated *in vivo* cross-linking of DNA with hMOF was performed with an hMOF-specific antibody as described previously (25, 69–71). Immunoprecipitated DNA from an equal number of control and irradiated cells was purified by the standard procedure. The yield of DNA was measured spectroscopically.

Immunofluorescence. Cell culture in chamber slides, fixation, and immunostaining were done as previously described (1, 28, 59). Fluorescent images of foci were captured as described previously (26). Sections through nuclei were captured, and the images were obtained by projection of the individual sections as recently described (48). The results shown are from three to four independent experiments. Cells with a bubble-like appearance or micronuclei were not considered for IR-induced focus analysis. For immunostaining of meiocytes, 8 to 12 weeks old male mice maintained at the Washington University School of Medicine, St. Louis, MO, were sacrificed by cervical dislocation. Freshly obtained testes were dissected in ice-cold minimal essential medium (MEM). Structurally preserved nuclei for immunostaining were prepared by mincing fresh tissue in MEM (Life Technologies). After removal of tissue pieces, the suspension was immediately mixed with fixative (3.7% formaldehyde, 0.1 M sucrose) and placed on a drop of hypotonic solution placed on precleaned slides. After air drying, slides were stored at −20°C until further use. Immunofluorescent staining was done as described previously (24, 67).

Microirradiation. Cells were grown on coverslips, microirradiated with a laser at 365 nm according to the described procedure (81) or with a laser at 405 nm in combination with Hoechst 33342, and then incubated at 37°C for 10 min. Preextraction was done with a buffer containing 0.5% Triton X-100 on ice for 20 min. Cells with and without preextraction were fixed with 4% paraformaldehyde, incubated with 0.5% of Triton X-100, blocked with bovine serum albumin (BSA), and incubated with specific antibody. Cells were washed with phosphate-buffered saline (PBS), incubated with anti-rabbit IgG-Texas Red, washed with PBS, and mounted with DAPI (4′,6-diamidino-2-phenylindole). For live cell imaging, cells were grown on glass coverslip-bottomed chamber slides and maintained at 37°C and 5% CO_2 during experiments.

hMOF retention assay. To determine the retention of MOF with DNA, 10^7 cells growing in exponential phase were irradiated and fixed with 4% formaldehyde at different times postirradiation. Total DNA from 10^7 cells, coimmunoprecipitated with MOF or retinoblastoma (Rb) antibody after *in vivo* cross-linking, was performed by the standard procedure described previously (69, 71). Immunoprecipitated DNA was purified by the standard phenol chloroform procedure (57), and DNA was quantified with a NanoDrop 2000 spectrometer (Thermo Scientific, Inc.). The amount of DNA retained by MOF is presented in arbitrary units of retention (MOF retention).

To determine how tightly hMOF is bound with DNA, cells with and without exposure to IR were washed with ice-cold PBS, and cell fractionation was carried out by four consecutive extractions with increasing detergent concentrations as described previously (5). The supernatants were collected at each step after extraction buffer treatment, and supernatants were cleared by centrifugation. The fractions were labeled as fractions I to IV. Pellets of about 10^7 cells were first resuspended in 150 μl of fractionation buffer A for 5 min on ice. (Fractionation buffer A contains 50 mM HEPES, pH 7.5, 150 mM NaCl, 1 mM EDTA, and 0.2% Nonidet P-40, supplemented with protease inhibitors [Sigma] and phosphatase inhibitors [10 mM NaF].) Fraction 1 from different samples was collected following centrifugation at $1,000 \times g$ for 5 min, and pellets were washed with the same buffer A. The supernatant was collected (fraction II); the nuclear pellets were treated for 40 min on ice with 150 μl of fractionation buffer B containing 0.5% Nonidet P-40, which was subjected to centrifugation at $16,000 \times g$ for 15 min; and supernatant was collected as fraction III. The remaining pellets are fraction IV, which were finally lysed in SDS-PAGE buffer and boiled for 5 min. From each fraction, equal aliquots derived from equivalent cell numbers were loaded on 10% SDS-PAGE gels and blotted as previously described (24, 25, 69, 71).

RESULTS

Proteins involved in IR-induced DDR are unaffected by hMOF depletion. Our initial interest in hMOF was motivated by its involvement in H4-Lys16 acetylation (H4K16ac) and its ability to alter higher-order chromatin structure into a relaxed conformation (72–74). This activity has been linked with transcriptional upregulation in *Drosophila* (73), as is evidenced by studies demonstrating that almost all active genes on the X

chromosome of *Drosophila* are associated with robust H4-Lys16 acetylation (22). Our recent studies have revealed that MOF inactivation or depletion in mammalian cells results in loss of H4K16ac, which correlates with loss of cellular proliferation (24). Since several studies have suggested that lack of DDR components is likely to be responsible for loss of cellular proliferation and that IR-induced DNA damage status correlates with cell survival, we determined whether depletion of hMOF downregulates any specific gene(s) involved in the mammalian DDR. We compared the RNA expression profile, using microarray analysis, in 293 cells with and without hMOF depletion. A significant reduction in H4K16ac levels after transfection with hMOF siRNA was observed after 72 h (see Fig. S1A in the supplemental material), whereas no change in H4K16ac levels was observed in cells depleted of another histone acetyltransferase Tip60 (see Fig. S1A and B in the supplemental material). While depletion of hMOF resulted in a significant downregulation of 600 genes and upregulation of 431 genes, none of these gene-encoded proteins is known to be involved in DDR, except XRCC4. (The complete microarray data can be found at http://www.ncbi.nlm.nih.gov/geo/query/acc.cgi?token=fryfbgoiuayiebu&acc=GSE20193.) Similarly, overexpression of hMOF in 293 cells significantly increased the expression of 92 genes and downregulated 39 genes, but there was no change in expression of genes encoding proteins involved in DNA DSB repair (http://www.ncbi.nlm.nih.gov/geo/query/acc.cgi?token=fryfbgoiuayiebu&acc=GSE20193).

Consistent with the repair gene transcriptional profiles, we found no significant reduction or increase in the level of known DNA DSB repair proteins (ATM, Ku70, Ku80, ligase IV, DNA-PKcs, Artemis, XLF1 [Cernunnos], NBS1, MRE11, Rad50, Rad51, Rad52, Rad54, BRCA1, BRCA2, XRCC2, XRCC3, Rad51B, Rad51C, Rad51D, XRCC1, 53BP-1, SMC1, MDC1, FANCD2, CHK2, CHK1, Tip60, hSSB1, hSSB2, H2AX, etc.) in hMOF-depleted cells (see Fig. S1C in the supplemental material). These results suggest that hMOF depletion does not affect the levels of the most commonly known DNA DSB repair proteins at the transcriptional level. However, the effect of hMOF depletion on DDR could be due to abrogation of posttranslational modifications of proteins involved in DNA damage repair (24). Since the best-characterized posttranslational modification induced by DNA damage is the phosphorylation of histone H2AX, which appears immediately postirradiation as foci that colocalize with repairosomes (58), we determined whether depletion of hMOF influences the kinetics of appearance of γ-H2AX foci.

hMOF knockdown delays the appearance of postirradiation γ-H2AX foci. To test whether hMOF-dependent H4K16ac is critical for DDR, IR-induced repair-associated focus formation was examined. Seventy-two hours posttransfection with hMOF siRNA, 293 cells were irradiated with 1.5 Gy. Cells with more than ~4 γ-H2AX foci were counted at different time points postirradiation. We monitored simultaneously the transfection of hMOF siRNA-Cy3, H4K16ac levels, and the frequency of cells with γ-H2AX foci postirradiation (Fig. 1A; see Fig. S2A and B in the supplemental material). Cells deficient in hMOF contained reduced levels of H4K16ac (Fig. 1Aa) and had a delayed appearance of IR-induced γ-H2AX foci (Fig. 1Ba) but did not show any delay in the disappearance of

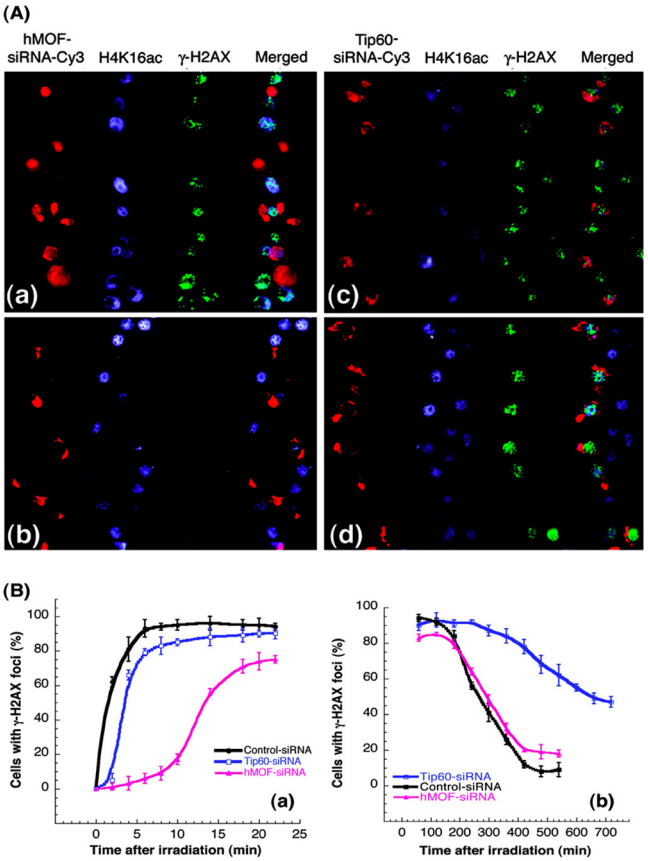

FIG. 1. Correlation between status of H4K16ac levels and IR-induced γ-H2AX focus formation in 293 cells. (A) Simultaneous detection of cells transfected with Cy3-labeled siRNA, H4K16ac status, and γ-H2AX focus appearance after exposure to 1.5 Gy of IR. (Aa and Ab) Cells were transfected with hMOF siRNA and analyzed for γ-H2AX foci after 5 min (Aa) and 300 min (Ab) of IR exposure. (Ac and Ad) Cells were transfected with Tip60 siRNA and analyzed for γ-H2AX foci after 5 min (Ac) and 300 min (Ad) of IR exposure. Panels Aa and Ac are magnified cells as shown in Fig. S2A and B in the supplemental material. (B) Frequency of cells with more than 2 γ-H2AX foci observed at various time points postirradiation. For each time point, 100 cells were analyzed. Each experiment was repeated three times; the mean numbers of cells with more than 2 foci are plotted against time. (a) Appearance of γ-H2AX foci in cells with and without depletion of either hMOF or Tip60. (b) Disappearance of γ-H2AX foci in cells with and without depletion of either hMOF or Tip60.

γ-H2AX foci once formed (Fig. 1Ab and Bb). Depletion of the histone acetyltransferase Tip60 has been shown to abrogate the disappearance of the damage-induced γ-H2AX variant in *Drosophila* (38). In agreement with that observation, we found that while depletion of Tip60 did not influence the levels of H4K16ac (see Fig. S1A and B in the supplemental material) and had minimal effect on the appearance of IR-induced γ-H2AX foci (Fig. 1Ac), it did induce a delay in the disappearance of γ-H2AX foci (Fig. 1Ad and Bb).

To determine whether depletion of hMOF also influenced the number of IR-induced γ-H2AX foci, the frequency of γ-H2AX foci per cell was quantified (see Fig. S2C and D in the supplemental material). hMOF-depleted cells have delayed induction of γ-H2AX focus formation (see Fig. S2C in the supplemental material). These results were similar to mouse

embryonic cells heterozygous for mouse Mof (mMof) (26), which had reduced induction of γ-H2AX foci. In contrast, Tip60 depletion had a minimal effect on initial IR-induced γ-H2AX foci, although such cells had a higher frequency of residual γ-H2AX foci per cell (see Fig. S2D in the supplemental material). The kinetics of appearance and disappearance of IR-induced γ-H2AX foci were similar with (Fig. 1B) and without (see Fig. S2C and D in the supplemental material) Cy3 labeling of hMOF siRNA.

hMOF and Tip60 have important but independent roles in the appearance and disappearance of γ-H2AX foci. Since hMOF depletion delayed the appearance of IR-induced γ-H2AX foci while Tip60 depletion delayed their disappearance, we determined how simultaneous depletion of hMOF and Tip60 altered γ-H2AX focus dynamics. Cells doubly depleted of hMOF and Tip60 showed similar kinetics of γ-H2AX focus appearance, as observed in cells only depleted of hMOF (see Fig. S3A in the supplemental material), and disappearance, as was observed in cells only depleted of Tip60 (see Fig. S3B in the supplemental material). These results suggest that hMOF and Tip60 have different nonoverlapping roles during IR-induced γ-H2AX focus appearance and disappearance.

Expression of a HAT-dead mutant hMOF (ΔhMOF) decreases IR-induced γ-H2AX focus formation. We have previously reported that overexpression of hMOF results in increased H4K16ac levels (24, 25) and that cells overexpressing hMOF show a slightly enhanced appearance of IR-induced γ-H2AX foci compared to control cells (see Fig. S4A in the supplemental material). These results suggest that any increase in the physiologically relevant levels of H4K16ac has a minimal effect on IR-induced γ-H2AX focus formation. To further investigate whether hMOF HAT activity is critical for IR-induced γ-H2AX focus formation, we determined whether ectopic expression of previously described construct of hMOF HAT-dead deletion mutant (ΔhMOF) (24, 25) abrogates IR-induced γ-H2AX focus formation. Endogenous expression of wild-type hMOF in cells expressing hemagglutinin (HA)-tagged ΔhMOF was knocked down by using a 3′UTR-specific hMOF siRNA. Cells expressing ΔhMOF had reduced levels of IR-induced γ-H2AX focus formation. Furthermore, ΔhMOF failed to rescue the defect in γ-H2AX focus formation brought on by depletion of endogenous wild-type hMOF (see Fig. S4B in the supplemental material), further supporting a role for H4K16ac status in IR-induced γ-H2AX focus formation.

Inhibition of histone deacetylase rescues IR-induced γ-H2AX focus appearance in hMOF-depleted cells. The above results support the argument that H4K16ac levels are critical for a timely DDR. To further confirm whether H4K16ac levels correlate with IR-induced γ-H2AX focus appearance, we used two different approaches. First we treated hMOF siRNA-transfected and control 293 cells with the histone deacetylase inhibitor trichostatin A (TSA) and determined the levels of H4K16ac. Cells treated with TSA had increased levels of H4K16ac without any change in hMOF levels (Fig. 2A). Cells with and without MOF depletion had higher levels of H4K16ac post-TSA treatment. Cells depleted of hMOF and treated with TSA had faster kinetics of IR-induced γ-H2AX focus appearance than untreated hMOF-depleted cells (Fig. 2B). This is consistent with the observation that TSA-treated hMOF-depleted cells also have enhanced growth rates (79). As tricho-

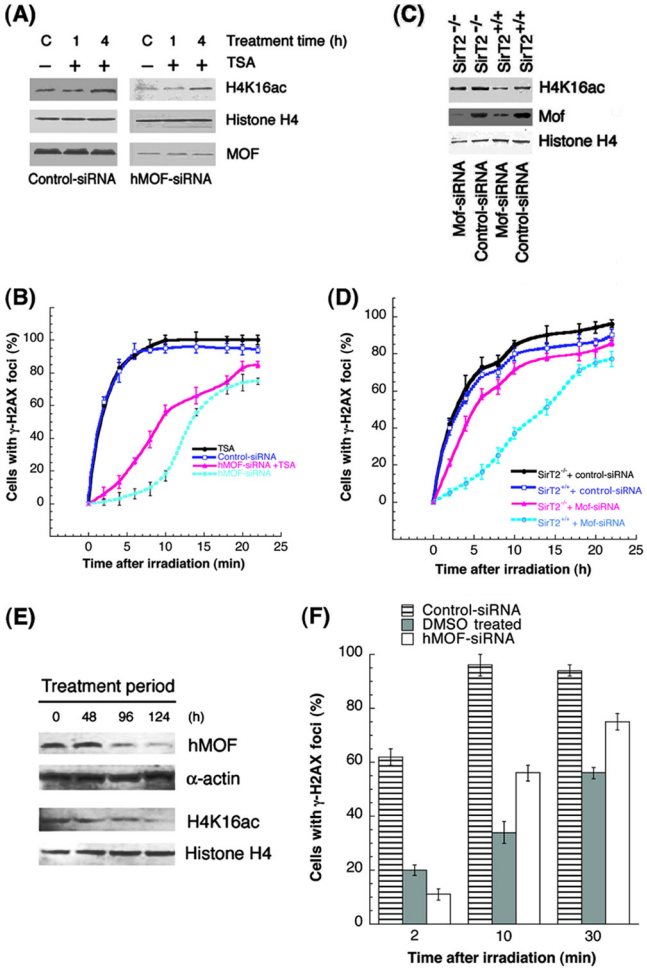

FIG. 2. Effect of H4K16ac levels on the appearance of IR-induced γ-H2AX foci. (A) 293 cells with and without knockdown of MOF were treated with TSA and examined for H4K16ac levels. Lane C, control. (B) Cells knocked down for hMOF and treated with TSA were irradiated and examined for appearance of γ-H2AX foci. (C) SirT2$^{+/+}$ and SirT2$^{-/-}$ mouse embryonic fibroblasts with knockdown of MOF, showing MOF and H4K16ac levels and (D) frequency of IR-induced γ-H2AX foci cells. (E) HL60 cells treated with DMSO for different time periods showing MOF, H4K16ac, and histone H4. (F) HL60 cells treated with DMSO or MOF knockdown and irradiated with 1.5 Gy, showing frequency of cells with γ-H2AX postirradiation.

statin A is known to inhibit several histone deacetylases, we wanted to determine whether the inactivation of SirT2, the major histone deacetylase (HDAC) (90), which deacetylates H4K16ac as well as H3K56ac (15), influences IR-induced γ-H2AX focus formation. SirT2-deficient cells had higher levels of H4K14ac than control cells expressing SirT2 (Fig. 2C), without showing any difference in the levels of MOF protein. Cells deficient for SirT2 had a modestly higher frequency of IR-induced γ-H2AX foci than cells with SirT2 (Fig. 2D). Depletion of MOF with siRNA in cells with and without SirT2 led to decreased MOF as well as H4K16ac levels (Fig. 2C). Interestingly, SirT2-deficient cells with knockdown of MOF showed relatively higher levels of H4K16ac compared to cells with SirT2 and depleted of MOF (Fig. 2D). Consistent with the levels of H4K16ac, cells with SirT2 and depleted of

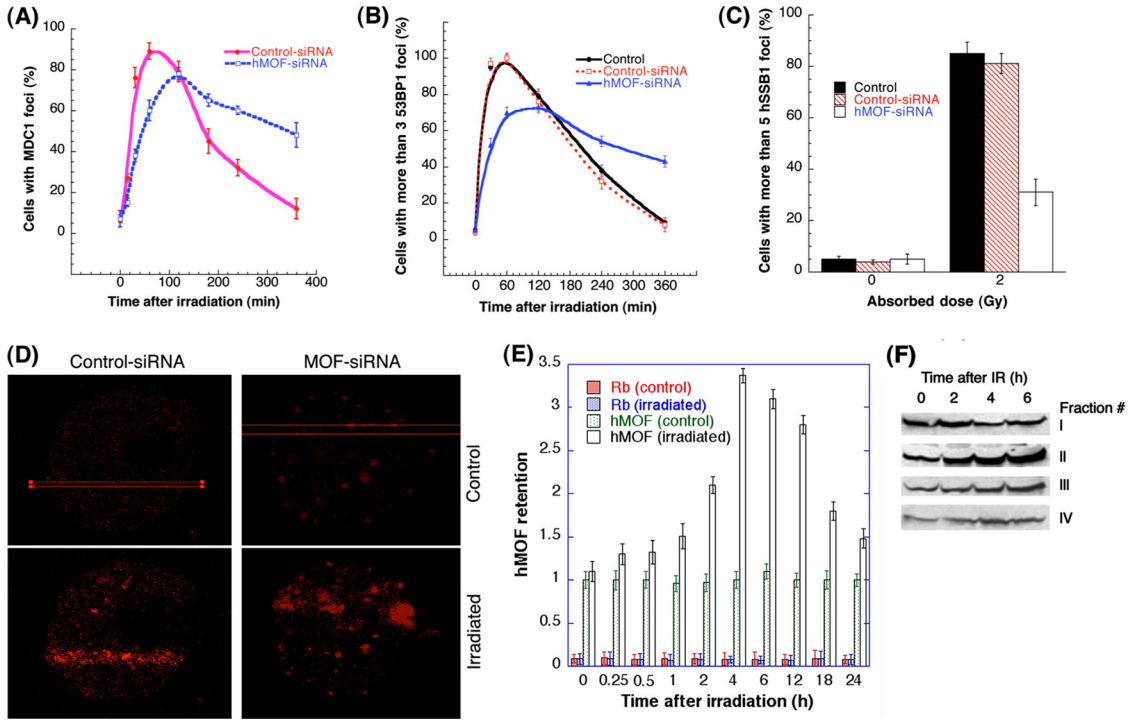

FIG. 3. hMOF depletion influences IR-induced repair focus-associated proteins and hMOF interaction with chromatin. 293 cells with and without depletion of hMOF with reduced levels of H4K16ac were irradiated with 6 Gy and quantified for foci at different time points postirradiation. (A) For MDC1, cells with more than 5 foci were counted. (B) For 53BP1, cells with more than 3 foci were counted. (C) For induction of hSSB1 foci, cells were irradiated with 2 Gy and cells with more than 2 foci were counted after 1 h postirradiation. (D) RFP-Rad52-expressing 293 cells knocked down for MOF were grown in the presence of bromodeoxyuridine (BrdU) and incubated in Hoechst 33342. Subnuclear DNA damage was induced in the designated rectangular boxes using a 405-nm laser on an LSM510 Zeiss confocal live-imaging system. (E) Association of hMOF with chromatin was determined by ChIP analysis. Cells were irradiated with 5 Gy and fixed, chromatin immunoprecipitation was performed with an hMOF or Rb antibody, and DNA was quantified by absorbance at 260 nm by NanoDrop 2000. (F) Cells with and without exposure to IR were analyzed for the retention of hMOF by Western blotting. hMOF was detected with a specific hMOF antibody.

MOF showed a longer delay in appearance of γ-H2AX foci compared to SirT2-deficient cells with MOF knockdown, which exhibited a minimal effect on IR-induced γ-H2AX focus formation (Fig. 2D), further supporting the role of H4K16ac in DDR.

We next determined the relationship between H4K16ac levels and cell proliferation in HL60 cells. Treatment of HL60 cells with dimethyl sulfoxide (DMSO) induces their differentiation and also reduces the levels of H4K16ac. A decrease in the levels of hMOF was also observed in cells treated with DMSO, whereas the levels of histone H4 did not change (Fig. 2E). After treatment with DMSO for 124 h, differentiated HL60 cells displayed a decreased frequency of γ-H2AX foci per cell following irradiation (Fig. 2F) as well as reduced telomerase activity (see Fig. S5 in the supplemental material), supporting the argument that decreased levels of H4K16ac correlate with defective DDR.

Inactivation of ATM in hMOF-depleted cells decreases IR-induced γ-H2AX focus formation. Ataxia-telangiectasia mutated (ATM) protein is an early responder to DNA damage with a key role in IR-induced phosphorylation of H2AX, and in the absence of ATM, H2AX is either phosphorylated by ATR or DNA-PKcs (10). Since, inactivation of ATM significantly delays IR-induced H2AX phosphorylation, we tested whether the formation of IR-induced γ-H2AX foci was affected by inactivating ATM in hMOF-depleted cells. Cells depleted of hMOF were treated with the ATM inhibitor, KU-55933, for 24 h and then examined for IR-induced γ-H2AX focus formation. We found that cells depleted with hMOF and treated with KU-55933 had a prolonged delay in the appearance of γ-H2AX foci when compared to cells only depleted of hMOF or cells only treated with KU-55933 (see Fig. S6A in the supplemental material). However, cells depleted of hMOF and treated with KU-55933 had a higher number of residual γ-H2AX foci than cells with only hMOF depletion (see Fig. S6B in the supplemental material).

hMOF and H4K16ac are important for the recruitment of key repair components to DNA damage sites. Chromatin marked by the phosphorylated form of H2AX becomes occupied by MDC1 (mediator of DNA damage-checkpoint protein 1) and 53BP1 (7). Therefore, we determined whether depletion of hMOF influences the frequency of focus formation of critical DDR components. First, we examined IR-induced MDC1 focus formation in cells with and without hMOF depletion. MDC1 is known to localize to sites of DNA DSB and is critical for DDR (40). Cells were treated with 5 Gy of IR and examined for MDC1 foci at increasing time intervals postirradiation. Cells depleted of hMOF had a reduced frequency of MDC1 foci and higher level of residual MDC1 foci postirradiation compared to control cells (Fig. 3A). A similar effect of

hMOF depletion was found for IR-induced 53BP1 focus appearance and disappearance (Fig. 3B).

We also tested whether hMOF influences IR-induced human single-stranded DNA binding protein (hSSB1) focus formation (62). hSSB1 accumulates in the nucleus and colocalizes with other known repair proteins but does not localize to replication foci in S-phase cells, and its deficiency does not influence S-phase progression (62). Since hSSB1 depletion abrogates the cellular response to DSBs (62), we determined whether hMOF depletion influences hSSB1 focus formation postirradiation. Cells irradiated with 2 Gy were examined for the frequency of hSSB1 foci 60 min postirradiation. The frequency of cells with hSSB1 foci was significantly lower in hMOF-depleted cells, supporting the role of hMOF in IR-induced DDR-associated focus formation (Fig. 3C). Furthermore, we determined in live cells whether depletion of MOF influences the recruitment of repair-associated Rad52 protein to damaged sites. Recruitment of red fluorescent protein (RFP)-Rad52 at a UV-laser-induced DNA damage site in cells with and without MOF depletion was analyzed at 10-min intervals up to 4 h postirradiation. Rad52 was observed to efficiently label the entire laser track, but in cells with MOF depletion and lower H4K16ac levels, labeling of the laser track was not detected (Fig. 3D). Such failure of Rad52 accumulation at damaged sites in MOF-depleted sites suggests that MOF facilitates the recruitment of Rad52 at damaged sites.

DNA damage stimulates hMOF association with chromatin. Our observations suggested that the delay in formation of IR-induced DNA DSB repair-associated foci seen in hMOF-depleted cells could be due to altered chromatin structure as a result of reduced basal-level H4K16ac. Additionally, we wanted to determine whether hMOF also contributes by altering chromatin structure during the process of DNA repair. Therefore, we determined whether hMOF is retained on DNA postdamage, as has been reported in the case of ATM (5). Cells were exposed to 5 Gy of IR and collected at different time points postirradiation, and chromatin immunoprecipitation was performed using hMOF or Rb antibody. hMOF association with DNA increased significantly at 2 h postirradiation, whereas no such change in Rb association was observed (Fig. 3E), suggesting that hMOF's ability to alter chromatin structure by acetylating H4K16 may be actively recruited and necessary for proper DNA repair and resetting the chromatin structure. To determine how tightly hMOF is associated with DNA postirradiation, we carried out cellular fractionation with successive detergent extractions to progressively remove loosely bound proteins. Since the increased association of hMOF with DNA was observed after 2 h of irradiation, we chose to analyze cells for the retention of hMOF at 2, 4, and 6 h postirradiation. Four fractions were collected from cells with and without irradiation. The first fraction (I) is the clarified cell extract collected after cells were treated with 0.2% Nonidet P-40-containing buffer. Fraction II is the extract from the cell pellet of the first fraction, which was washed again in 0.2% Nonidet P-40-containing buffer. Fraction III contains a longer extraction with 0.5% Nonidet P-40 which was carried out on the remaining pellet from the second fraction. Fraction IV contains the insoluble remains that were boiled in electrophoresis sample buffer. Consistent with the ChIP data, fractions II to IV showed consistently increased retention of hMOF in treated samples compared to untreated cells at 2 h postirradiation (Fig. 3F).

Decreased MOF and H4K16ac abrogate γ-H2AX focus formation at a defined DNA DSB site. To establish a direct link between H4K16ac status and H2AX phosphorylation at the site of DNA DSB, we used the system in which a single DSB is induced at a defined genomic site in NIH 3T3-derived cell lines (77). These cells (NIH2/4) were engineered to contain a single copy of the 18-nucleotide I-SceI restriction site flanked on one side by an array of 256 copies of the *lac* repressor binding site and on the opposite side by 96 copies of the tetracycline response element (77). The I-SceI restriction endonuclease tagged with the ligand-binding domain of the glucocorticoid receptor (I-SceI-GR) remained cytoplasmic in the absence of triamcinolone acetonide (TA), and DNA DSBs were not detected when noninduced cells were immunostained with antibody specific to γ-H2AX. Treatment with TA induced translocation of I-SceI to the nucleus and rapid induction of a single DNA DSB, as visualized by detection of a single nuclear γ-H2AX focus by immunofluorescence (Fig. 4A). NIH2/4 cells depleted of MOF by MOF siRNA (Fig. 4B) showed a delay in the appearance of the TA-induced γ-H2AX focus (Fig. 4C). These kinetics were similar to those seen in cells irradiated with IR (Fig. 1).

NIH2/4 cells with and without MOF depletion were treated with TA and analyzed for MOF as well as H4K16ac status. Cells treated with TA were fixed at different time points after TA treatment, and quantification of MOF- and H4K16ac-bound DNA was done by fluorescent intensity (Fig. 4A; see Fig. S7 in the supplemental material) and real-time PCR (Fig. 4D). The fluorescent intensity measurement of γ-H2AX, MOF, and H4K16ac at and around the I-SceI DSB site revealed that the accumulation of γ-H2AX peaked at the DSB site, whereas MOF and H4K16ac levels did not change around the DNA DSB (Fig. 4A). We found that cells depleted of hMOF had reduced numbers of γ-H2AX foci, which correlated with reduced global levels of H4K16ac (see Fig. S8 in the supplemental material). Thus, the delayed appearance of γ-H2AX foci following knockdown of MOF appears to be correlated with the globally decreased levels of H4K16ac, suggesting that H4K16ac has a role in DNA DSB-induced γ-H2AX focus formation (see Fig. S8 in the supplemental material). However, chromatin immunoprecipitation (62, 64) revealed that the levels of MOF as well as H4K16ac present at the I-SceI (bp 94 to 378) site did not change following induction of I-SceI-induced DSB (Fig. 4D). These results suggest that DNA DSB does not induce changes of MOF and H4K16ac levels at the site of damage.

hMOF depletion alters DNA DSB repair by NHEJ. We determined whether depletion of hMOF and lack of H4K16ac altered non-homologous end-joining-mediated DNA DSB repair. In the first assay, we performed ligation-mediated (LM)-PCR using the approach described in reference 77 and found that NIH2/4 cells depleted of MOF displayed delayed DSB repair, which is consistent with the observation of the delayed appearance of γ-H2AX foci. We further supported these findings by using an engineered cell line that can express the red fluorescent protein (RFP) only upon repair of I-SceI-induced DSBs by NHEJ (Fig. 4E). Depletion of MOF resulted in a decreased number of cells with RFP (Fig. 4F). These data

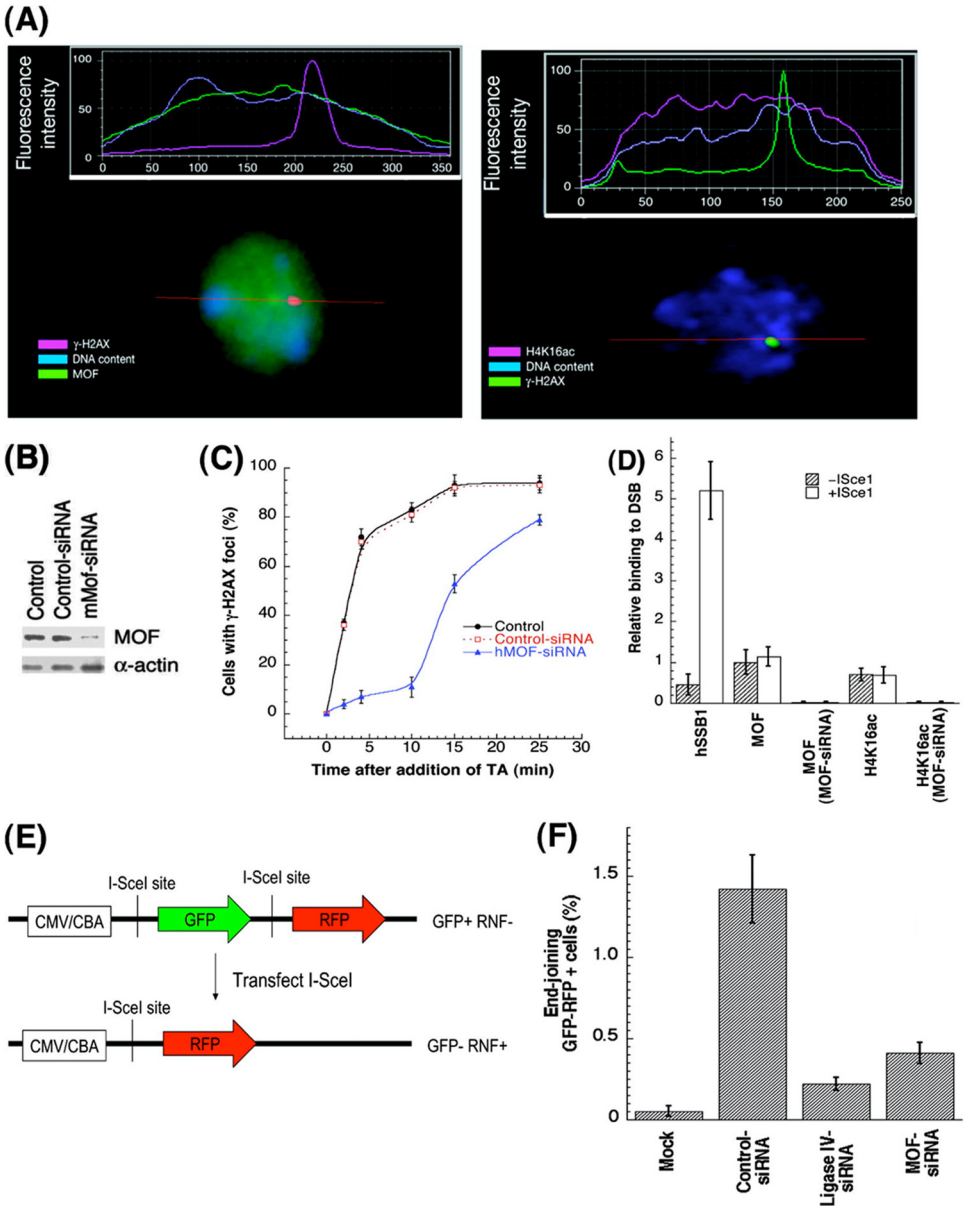

FIG. 4. MOF depletion results in delayed appearance of γ-H2AX focus at a site-specific DNA DSB. (A) Mouse NIH2/4 cells with and without treatment with TA were fixed and examined for the presence of a γ-H2AX focus. The fluorescence of γ-H2AX, MOF, and DNA was measured across the nucleus and plotted on the top of the cell nucleus. Immunofluorescence was performed with anti-γ-H2AX, anti-H4K16ac, and anti-MOF antibody, and cells were counterstained with DAPI. Fluorescent intensities were measured using Isis or Zen software for each channel. (B) Western blot detection of MOF 72 h posttransfection with siRNA in NIH2/4 cells. (C) NIH2/4 cells with and without MOF depletion were treated with TA and fixed at different time points to detect a γ-H2AX focus by immunostaining. (D) ChIP analysis in I-SceI-induced cells with and without knockdown of MOF examined for bound MOF, H4K16ac, and histone H4. No changes of MOF and H4K16ac levels at the site of damage were detected. (E and F) Effect of MOF on NHEJ. (E) 293 engineered cell line that can become fluorescent (RFP) only upon repair of I-SceI-induced DSBs by NHEJ. CMV, cytomegalovirus; CBA, chicken β-actin promoter. (F) Depletion of MOF results decreased frequency of cells with RFP. These data clearly indicate that the cell's H4K16ac status plays a critical role in the NHEJ pathway.

clearly indicate that the cell's H4K16ac status plays a critical role in the NHEJ pathway.

hMOF interacts with DNA-PKcs: hMOF depletion abrogates IR-induced ATM-dependent DNA-PKcs phosphorylation. The above results indicate that MOF is involved in the NHEJ pathway. In order to determine whether MOF physically interacts with proteins directly involved in DNA DSB, we performed a general search for hMOF-interacting proteins using a tandem-affinity-purification (TAP)-tagged hMOF expressed in human cells. Proteins copurifying with MOF were identified by mass spectrometry and confirmed by Western blotting. hMOF is a component of both hMOF-host cell factor (HCF)-hMSL1v-hNSL and hMOF-hMSL1/2/3 complexes, while hMSL3 is only a component of hMOF-hMSL1/2/3 complexes (11, 39, 42, 75). The Western blot analysis indicates that DNA-PK is more associated with the hMOF-hMSL1v-HCF

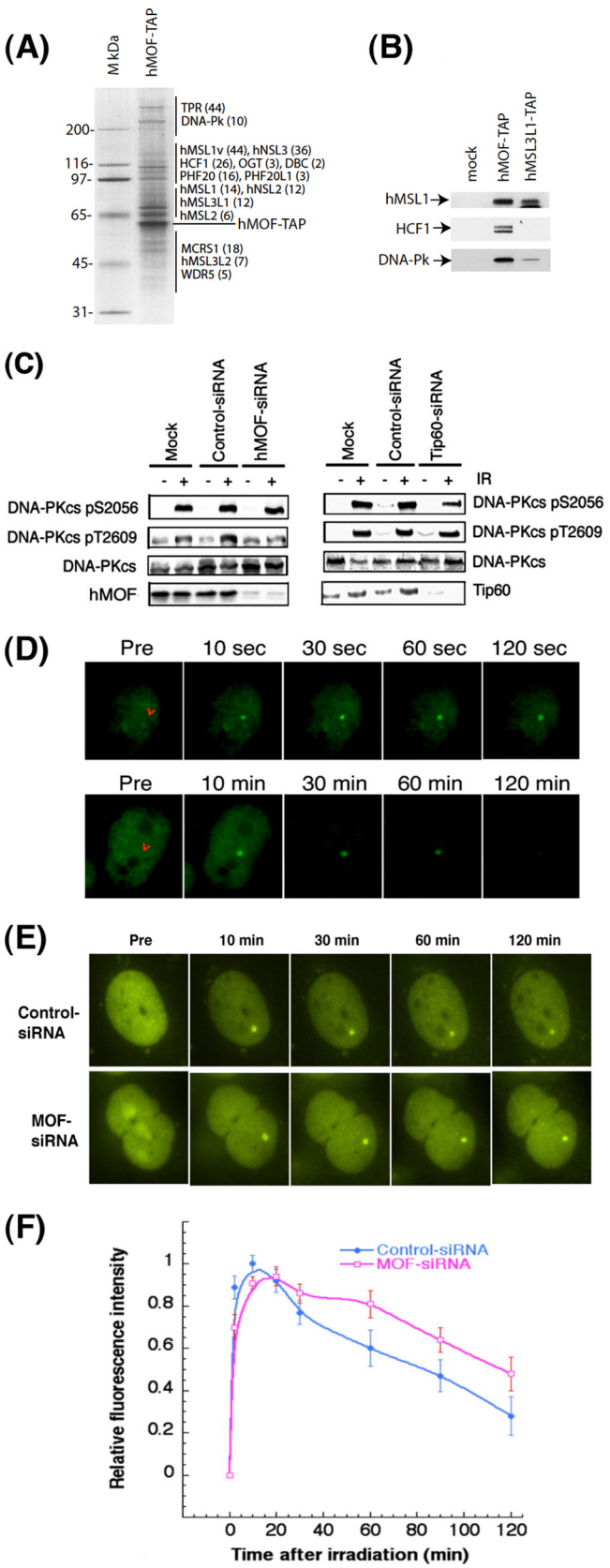

FIG. 5. Interaction of hMOF with DNA-PKcs. (A) hMOF-TAP is purified with distinct sets of associated proteins. The calmodulin fraction of hMOF-TAP was separated by SDS-PAGE and stained with Sypro Ruby Red, and gel slices were subjected to in-gel digestion and mass spectrometry. M, molecular mass marker. Peptides corresponding to hMSLs and other proteins were identified (numbers of peptides are shown in parentheses) (see Fig. S9 in the supplemental material). DNA-PKcs copurifies preferentially with hMOF. hMOF TAP-, hMSL3L1 TAP-, and mock TAP-purified fractions were assayed for the presence of hMSL1, HCF-1, and DNA-PKcs by Western blotting (B). (C) Cells with and without depletion of hMOF or Tip60 were irradiated with 5 Gy and examined for DNA-PKcs phosphorylation using antibodies specific for pS2056 and pT2609. Depletion of hMOF resulted in loss of ATM-dependent phosphorylation of DNA-PKcs (pT2609), and no such loss was observed in Tip60-depleted cells. (D) Recruitment of DNA-PKcs to the laser-induced DNA DSBs. Cells were transfected with YFP-DNA-PKcs and microirradiated. Time-lapse imaging of YFP-DNA-PKcs-expressing U2OS cells was done before and after microirradiation. (E) Cells stably expressing YFP-DNA-PKcs were treated with control or hMOF siRNA for 72 h, and microirradiated. (F) Initial accumulation kinetics (see Fig. S9B in the supplemental material) and relative fluorescence for a 2-h time course of treatment with YFP-DNA-PKcs at laser-generated DSBs. Error bars represent the standard deviations (SD) from three different experiments.

complex than with the hMSL complex (Fig. 5). In contrast to the purified hMOF-hMSL complex obtained using TAP-tagged hMSL3L1, the pattern of bands obtained with hMOF-TAP was less clear, with hMOF-TAP being by far the most prominent band (Fig. 5). This result indicates that hMOF can associate with polypeptides other than the conserved MSL proteins: for instance, with host cell factor 1 (HCF-1) (Fig. 5). We confirmed that HCF-1 associates specifically with hMOF by performing Western blot analysis with an anti-HCF antibody on hMOF TAP-, hMSL3L1 TAP-, and mock TAP-purified samples (Fig. 5B). These data clearly indicate that hMOF associates with HCF-1 in a complex distinct from the hMSL complex obtained with hMSL3L1.

Additionally hMOF was found to copurify with a significant amount of DNA-dependent protein kinase catalytic unit (DNA-PKcs) (Fig. 5A and B; see Fig. S9A in the supplemental material). The activity of this serine/threonine protein kinase is stimulated by its recruitment to the DNA DSB via the Ku heterodimer, Ku80/Ku70. Since DNA-PKcs is critical for DNA repair via the NHEJ pathway and also plays a role in the signaling response to DNA damage (58, 68), we determined whether depletion of hMOF influences IR-induced phosphorylation of DNA-PKcs. Cells depleted of hMOF had decreased ATM-dependent IR-induced DNA-PKcs phosphorylation at the pT2609 site but not at the pS2056 DNA-PKcs autophosphorylation site (Fig. 5C). In contrast, Tip60 depletion had no effect on IR-induced DNA-PKcs phosphorylation at T2609. These results suggest that hMOF is critical for the activation of DNA-PKcs.

We further determined the impact of hMOF on DNA-PKcs accumulation at DSB sites by using live cell imaging combined with microirradiation of cells expressing yellow fluorescent protein (YFP)-tagged DNA-PKcs. We observed a modest increase in the YFP-tagged DNA-PKcs accumulation at the site of damage (Fig. 5D). To determine the influence of hMOF depletion on DNA-PKcs accumulation at the site of damage, cells were irradiated and time-lapse imaging to monitor YFP intensity was performed (Fig. 5D). Cells depleted of hMOF

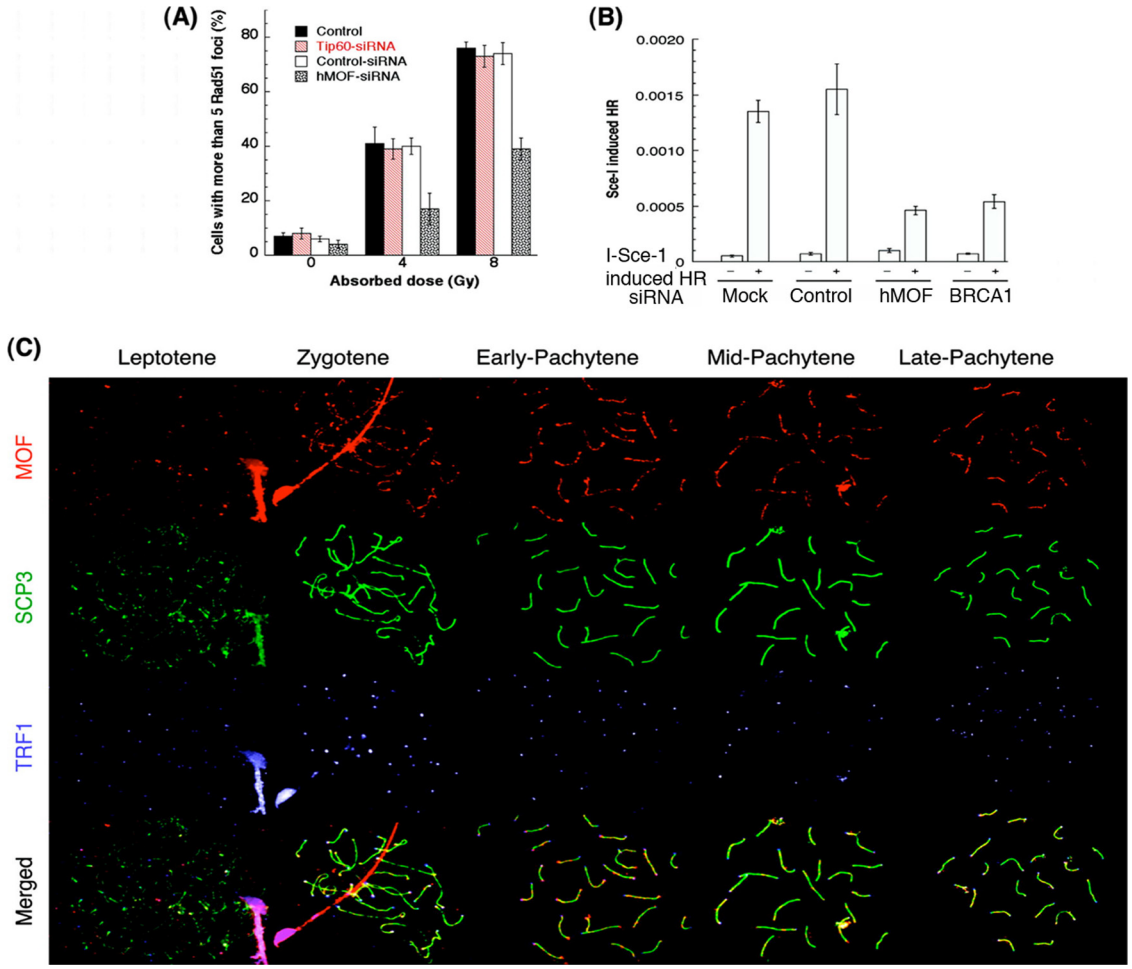

FIG. 6. MOF plays a role in HR. (A) Cells with and without MOF or Tip60 knockdown were irradiated with different doses, and cells were quantified for the presence of Rad51 foci after 4 h of irradiation. (B) Impairment of I-SceI-induced HR in hMOF-deficient cells was found. HR frequencies are shown with (+) or without (−) I-SceI induction in untreated cells, in cells treated with control siRNA, and in cells treated with hMOF- or BRCA1-specific siRNA (54). The results presented are the mean and standard error from three independent experiments. (C) Localization of MOF on mouse meiotic chromosomes during prophase 1. Spermatocyte spreads from male mice were immunostained with anti-MOF, anti-TRF1, and anti-SCP. MOF is in red, synaptonemal complex protein SCP3 is green, and TRF1 is white on chromosomes from mouse spermatocytes. The presence of MOF on synaptonemal complexes from leptotene to mid-pachytene suggests the role of MOF in meiotic recombination.

showed slower kinetics of the appearance as well as disappearance of fluorescent focus (Fig. 5E and F; see Fig. S9B in the supplemental material). These results suggest that hMOF depletion influences IR-induced ATM-dependent DNA-PKcs phosphorylation as well as its accumulation at the sites of damage (Fig. 5F).

hMOF depletion alters DNA DSB repair by the HR pathway. DNA DSBs are repaired by either the NHEJ or HR pathways (13, 27, 31, 65, 68, 76). Homologous recombination requires a sister chromatid, homolog, or homologous sequence on a heterolog to be used as a template for DNA DSB repair and thus requires more significant chromatin remodeling and greater DNA accessibility to facilitate DNA unwinding, strand invasion, and DNA replication-based repair mechanisms. We investigated the role of hMOF in HR repair by first examining the effect of hMOF depletion on Rad51 focus formation.

The Rad51 protein is a central player in homolog-directed recombinational repair (58, 63). It localizes to a homologous sequence and forms initial joints, even on the surface of nucleosomes (63). Similarly, Rad51 also colocalizes with γ-H2AX and Dmc1 foci on synaptonemal complexes at the leptotene and zygotene stages of meiosis, where recombination events also take place (20). Cells with and without hMOF depletion were irradiated with different doses of IR, and Rad51 foci were examined 3 h after irradiation. Depletion of hMOF reduced the frequency of cells with IR-induced Rad51 foci (Fig. 6A), suggesting that hMOF has a role in the repair of DNA DSB by HR.

Since hMOF depletion decreases hSSBI foci (Fig. 3C) as well as Rad51 focus formation (Fig. 6A), and both proteins have a role in HR, we directly determined the influence of hMOF on HR by two different approaches. In the first approach, cells depleted of hMOF were treated with mitomycin C and examined for sister chromatid exchanges (SCEs) by the previously described procedure (49, 51). Mitomycin C treatment increased the frequency of SCEs, reflecting increased

recombination frequency. Cells depleted for hMOF showed a decreased frequency of mitomycin C-induced SCEs (see Fig. S10 in the supplemental material), suggesting defective recombination. To further test whether HR is affected, we examined the reconstitution frequency of a GFP reporter gene within a chromosomally integrated plasmid substrate (61) in cells with or without reduced levels of hMOF. Following I-SceI transfection, the population of cells containing the pDR-GFP substrate demonstrated a >80-fold increase in the number of GFP-positive members compared with cells containing the control vector, indicating that almost all of the GFP-positive cells resulted from DSB-induced recombination. pDR-GFP cells treated with hMOF siRNA had an ~3-fold reduction in the number of GFP-positive cells in comparison to control siRNA-transfected cells (*t* test; $P < 0.001$) (Fig. 6B). These data along with the observation of reduced frequency of Rad51 foci and inefficient recruitment of Rad52 on the damaged chromatin provide strong evidence that hMOF affects the HR pathway for DNA DSB repair.

Further validation for a role of MOF in DNA DSB repair by HR was obtained by analysis of this HAT in meiotic cells, which are programmed for homologous recombination. Since meiotic recombination is initiated by DSBs that are introduced into leptotene DNA by the conserved SPO11 transesterase (33, 41), we determined the localization of MOF during the leptotene-to-pachytene stages of male meiosis in the testes of mice. Interestingly, MOF was found associated with the synaptonemal complexes through the progression of pairing and synapsis of the homologous chromosomes in the first meiotic division from leptotene to late pachytene (Fig. 6C). This confined localization of MOF to the chromatin domains undergoing active pairing and recombination further argues that MOF has a role in DNA DSB meiotic recombination. Taken together, the present data suggest that MOF plays a functional role in the process of homologous recombination.

DISCUSSION

We sought to determine whether the ubiquitous, preexisting basal levels of H4K16 acetylation have a role in DDR and what impact H4K16ac's absence may have on DNA DSB repair by NHEJ or HR pathways. Our results provide strong evidence that preexisting H4K16ac does facilitate DNA damage recognition (Fig. 7). Based on the established role of this modification in chromatin organization, our observations are consistent with the model wherein basal levels of H4K16ac maintain a chromatin structure conducive for efficient DNA damage repair. This model (Fig. 7) is based on the fact that specifically altering the levels of H4K16ac by various approaches directly affected IR-induced γ-H2AX focus formation: (i) MOF depletion reduced H4K16ac levels and delayed/abrogated IR-induced focus formation of γ-H2AX, MDC1, 53BP1, Rad51, and hSSB1; (ii) depletion of Tip60, another HAT, had no impact on H4K16ac levels and no influence on γ-H2AX focus formation; (iii) depletion of Tip60 did not enhance the delay in the IR-induced γ-H2AX focus formation in cells depleted for hMOF; (iv) cells expressing HAT-dead MOF had a delay in the appearance of IR-induced γ-H2AX focus formation; (v) treatment of cells with TSA enhanced H4K16ac levels and reversed the delay in γ-H2AX focus formation upon depletion of hMOF; (vi) MOF depletion had a minimal effect on the appearance of IR-induced γ-H2AX foci in SirT2$^{-/-}$ cells as compared to SirT2$^{+/+}$ cells; and (vii) MOF depletion along with ATM inactivation increased the delay in the formation of IR-induced γ-H2AX foci.

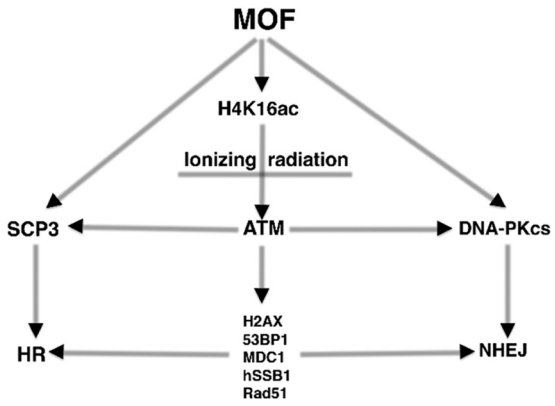

FIG. 7. MOF and H4K16ac influence DDR at multiple stages of DNA DSB repair pathways. MOF is a major HAT for H4K16ac, and its levels determine IR-induced repairosome formation. MOF interacts with DNA-PKcs and also localizes on the synaptonemal complex (SCP3) of meiocytes, thus linking to both the DNA DSB repair pathways.

Our comprehensive analysis of the correlation between the chromatin modifier MOF, modified histone H4 residue K16ac, and IR-induced DDR strongly supports the argument that acetylation of histone H4K16 strongly influences DDR (Fig. 7). The role of H4K16ac in DDR is further supported by the fact that the acetylation at the N-terminal tails of histones H3 and H4 correlates with the establishment of an open euchromatin conformation that is transcriptionally active. Conversely, hypoacetylation of H3 and H4 tails is associated with heterochromatin (36, 89). Our results argue that the two different forms of chromatin could differentially influence generation of DDR-associated signaling. Histone acetylation impacts chromatin structure through the neutralization of the positive charges on lysine residues, altering intra- and internucleosomal interactions of the chromatin fiber and thus facilitating decondensation and enhancing nucleosomal DNA accessibility (6, 35). It is well established that histone acetylation is recognized by transcriptional factors or ATP-dependent remodeling activities (91), but since acetylated K16 (H4K16ac) is present in ~60% of the total H4 molecules of mammalian cells (84), it is likely that it also has a specific structural role in chromatin-based processes such as DDR. Shogren-Knaak and coworkers have demonstrated the structural significance of histone H4 at lysine 16 (H4K16ac) as its incorporation into nucleosomal arrays abrogates the formation of compact 30-nm-like fibers (74). The adaptor protein 14-3-3 binds the phosphorylated nucleosome and recruits MOF, which triggers the acetylation of histone H4 at lysine 16 (94). Nucleosomes with H4K16ac in the fiber have a decreased ability to form cross-fiber interactions (74), and thus the chromatin remains in an open state, conducive to DDR. This assumption is consistent with the fact that H4K16ac levels peak in S phase (91), the cell cycle phase most efficient for DNA DSB repair and which has less IR-induced

cell killing than during the G_1 and G_2 phases of the cell cycle (55, 56).

Histone acetyltransferases exist as components of multisubunit protein complexes involved in different processes such as transcription activation, gene silencing, and cell cycle progression as well as DNA damage repair (12). Such complexes have been reported to contain ATM-related proteins such as TRRAP, which is found in human Tip60 and PCAF complexes (3). ATM is implicated in mitogenic signal transduction, chromosome condensation, meiotic recombination, cell cycle control, and telomere maintenance (50, 52, 53).

The effect of MOF on ATM activation is by an indirect mechanism, and inactivation of ATM or p53 does not rescue lethality due to MOF deletion (24). In addition, our current studies reveal that depletion of MOF does not influence the levels of proteins known to be involved in DDR, suggesting that MOF-dependent H4K16ac primarily affects DDR through a direct impact on chromatin structure (Fig. 7). Given the significance of H4K16ac, its absence could result in reduced transmission of signals generated from DNA damage sites, and this would delay the timely course of repair. Furthermore, analysis of H4K16ac levels at the site of I-SceI-induced DSB in MOF-depleted cells revealed a direct correlation between loss of H4K16ac and abrogation of γ-H2AX focus appearance.

In addition to histone kinases, several studies have revealed the role of HAT complexes in DNA DSB repair. It has been reported that HAT complexes act in concert with the ATP-dependent SWI/SNF and RSC (which remodels the structure of chromatin)-containing chromatin-remodeling complexes to facilitate DNA repair (58). Cells expressing catalytically inactive TIP60 have been found to have impaired DNA DSB repair (30). TIP60 with its cofactor TRRAP directly binds to chromatin near DNA DSBs, and depletion of TRAPP impairs DNA damage-induced H4 acetylation, which results in defective DSB repair by HR (45). Similar results were observed with NuA4, a yeast homolog of TIP60, following induction of DSB by HO endonuclease (17). NuA4 binds directly to sites of DNA DSBs concomitantly with the appearance of γ-H2AX (17).

Our analysis revealed that MOF influences the formation of DNA DSB repair-associated foci, but its global association with chromatin increases postirradiation, as determined by ChIP assay (Fig. 3E). Furthermore, MOF retention on chromatin also increases postirradiation, suggesting that MOF itself has a critical role in the later steps of DNA DSB repair, which is evidenced by the fact that cells expressing mutant MOF had higher residual DNA DSBs and chromosome aberrations (25). Our previous studies have revealed that expression of mutant hMOF induced neither a significant increase in G_1-phase cells nor a decrease in S-phase entry or accumulation in G_2 phase after IR exposure compared to control cells (25, 75). However, cells expressing a HAT-dead mutant of hMOF had a higher frequency of IR-induced chromosomal aberrations, suggesting that hMOF does influence DNA DSB repair (25).

Further evidence for the role of MOF in DNA DSB repair is provided by the following observations: (i) MOF forms a complex with DNA-PKcs, and (ii) MOF localizes on the synaptonemal complexes in spermatocytes. Depletion of MOF resulted in abrogation of IR-induced ATM-dependent phosphorylation of DNA-PKcs. These observations are consistent with the model proposed earlier that MOF regulates the ATM function through the status of chromatin (Fig. 7). Furthermore, depletion of MOF delays the accumulation of DNA-PKcs postirradiation. Delay in the accumulation could be due to following reasons: (i) loss of ATM-dependent damage-induced DNA-PKcs phosphorylation; (ii) change in chromatin structure due to loss of H4K16ac; and (iii) decreased association of MOF with DNA postirradiation, preventing chromatin alterations conducive for DSB repair.

hMOF functions upstream of ATM (25), possibly sensing DNA damage-induced chromatin changes with subsequent signaling to ATM effectors. In contrast, Tip60 has been reported to activate ATM by acetylation of its lysine residue, and so ATM activation could be independent of chromatin modifications (78). Overall, histone acetylation appears to both unwind chromatin and create a permissive platform that facilitates recruitment of remodeling complexes. The INO80 complex, including the INO80 member of the SWI/SNF family, has long been known to regulate transcription at RNA polymerase II (Pol II) promoters through chromatin remodeling. More recently, it was observed that INO80 is recruited to γ-H2AX near DNA DSBs, and yeast mutants of INO80 are hypersensitive to damaging agents and HO endonuclease, providing one of the first examples of SWI/SNF ATPase participation in DNA repair (44, 60, 86). Interestingly, the actin-related protein Arp4 in yeast is present in both the NuA4-HAT complex and the INO80-SWR1 complex, further suggesting concerted action of histone-modifying and chromatin-remodeling activities in the DSB response (17). The exact role of INO80 has yet to be clearly defined. TRRAP-TIP60 activity may be limited to local chromatin unwinding since chromatin relaxation alone is sufficient to rescue the defects caused by TRRAP deficiency (45). Since the role of MOF through alteration of H4K16ac levels is upstream in DDR and MOF forms a complex with DNA-PKcs, essential for NHEJ, our studies also found that MOF is required for the repair of DNA DSB by the HR pathway. This is supported by the observations that depletion of MOF results in the abrogation of Rad51 focus formation (Fig. 6A) and reduced frequency of sister chromatid exchange formation (see Fig. S10 in the supplemental material). Further evidence about the role of MOF comes from the following observations: (i) depletion of MOF results in reduced frequency of I-SceI-induced DSB repair, and (ii) MOF is localized on the synapetonemal complex during the process of meiotic recombination.

In contrast to yeast, which has only two copies of histone H4, studying the direct role of lysine 16 of histone H4 in mammalian cell systems is more difficult due to the presence of multiple copies of the H4 gene. Moreover, the yeast and mammalian systems are substantially different, since deletion of Sas2, the main H4K16 acetyltransferase in yeast, does not result in cellular lethality, whereas deletion of MOF not only results in embryonic lethality but also has a cytostatic effect in many human and mouse cell lines examined (24). Although loss of acetylation at H4K16 does influence transcription in both yeast (14, 16) and mammalian (32, 90, 91) cells, it is important to note that chromatin modifications common to yeast and mammalian systems do not always lead to similar DDR phenotypes. Acetylation of H4K16, for example, results in loss of histone H4 in yeast but does not result in loss of histone H4 in mam-

malian cells. This could be due to the fact that mammalian cells have a much more complex chromatin organization, so that H4K16ac could be playing a more critical role in DDR, as is further supported by the present work.

In summary, these data indicate that H4K16ac (histone code) constitutes one of the main early signals for generation of efficient DDR, which influences both of the pathways of DNA DSB repair. These results are consistent with the finding that chromatin alterations due to DNA DSB trigger ATM phosphorylation in mammalian cells, which is abrogated when cells are depleted of MOF. Abrogation of both DNA DSB repair pathways at several stages in cells depleted of MOF and the presence of MOF in the synaptonemal complex are further strong evidence of the role of MOF in DDR. Since MOF is indispensable for both NHEJ and HR DNA DSB repair pathways, H4K16ac (a histone code) must provide a permissive chromatin environment critical for DDR and subsequent mammalian cell survival. Further studies should reveal whether the H4K16ac levels of any particular region of the genome are critical for DDR.

ACKNOWLEDGMENTS

We thank Fred Alt for SirT2 mouse embryonic fibroblast cells and Tom Misteli for reagents. Thanks are due to Clayton Hunt, Sandeep Burma, Nobuo Horikoshi, and the members of the Pandita laboratory for suggestions and comments and helpful discussion.

This work was supported by grants NIH CA123232 and CA10445 to T.K.P.; CA 50519 to D.C.; and CIHR MOP-64289 to J.C., who is also a Canada Research Chair. N.A. is a CIHR postdoctoral fellow.

We declare that we have no competing financial interests.

REFERENCES

1. **Agarwal, M., S. Pandita, C. R. Hunt, A. Gupta, X. Yue, S. Khan, R. K. Pandita, D. Pratt, J. W. Shay, J. S. Taylor, and T. K. Pandita.** 2008. Inhibition of telomerase activity enhances hyperthermia-mediated radiosensitization. Cancer Res. **68:**3370–3378.
2. **Akhtar, A., and P. B. Becker.** 2000. Activation of transcription through histone H4 acetylation by MOF, an acetyltransferase essential for dosage compensation in Drosophila. Mol. Cell **5:**367–375.
3. **Allard, S., R. T. Utley, J. Savard, A. Clarke, P. Grant, C. J. Brandl, L. Pillus, J. L. Workman, and J. Cote.** 1999. NuA4, an essential transcription adaptor/histone H4 acetyltransferase complex containing Esa1p and the ATM-related cofactor Tra1p. EMBO J. **18:**5108–5119.
4. **Allfrey, V. G., B. G. Pogo, V. C. Littau, E. L. Gershey, and A. E. Mirsky.** 1968. Histone acetylation in insect chromosomes. Science **159:**314–316.
5. **Andegeko, Y., L. Moyal, L. Mittelman, I. Tsarfaty, Y. Shiloh, and G. Rotman.** 2001. Nuclear retention of ATM at sites of DNA double strand breaks. J. Biol. Chem. **276:**38224–38230.
6. **Anderson, L., C. Henderson, and Y. Adachi.** 2001. Phosphorylation and rapid relocalization of 53BP1 to nuclear foci upon DNA damage. Mol. Cell. Biol. **21:**1719–1729.
7. **Bekker-Jensen, S., C. Lukas, R. Kitagawa, F. Melander, M. B. Kastan, J. Bartek, and J. Lukas.** 2006. Spatial organization of the mammalian genome surveillance machinery in response to DNA strand breaks. J. Cell Biol. **173:**195–206.
8. **Bird, A. W., D. Y. Yu, M. G. Pray-Grant, Q. Qiu, K. E. Harmon, P. C. Megee, P. A. Grant, M. M. Smith, and M. F. Christman.** 2002. Acetylation of histone H4 by Esa1 is required for DNA double-strand break repair. Nature **419:**411–415.
9. **Botuyan, M. V., J. Lee, I. M. Ward, J. E. Kim, J. R. Thompson, J. Chen, and G. Mer.** 2006. Structural basis for the methylation state-specific recognition of histone H4-K20 by 53BP1 and Crb2 in DNA repair. Cell **127:**1361–1373.
10. **Burma, S., B. P. Chen, M. Murphy, A. Kurimasa, and D. J. Chen.** 2001. ATM phosphorylates histone H2AX in response to DNA double-strand breaks. J. Biol. Chem. **276:**42462–42467.
11. **Cai, Y., J. Jin, S. K. Swanson, M. D. Cole, S. H. Choi, L. Florens, M. P. Washburn, J. W. Conaway, and R. C. Conaway.** 2010. Subunit composition and substrate specificity of a MOF-containing histone acetyltransferase distinct from the male-specific lethal (MSL) complex. J. Biol. Chem. **285:**4268–4272.
12. **Carrozza, M. J., R. T. Utley, J. L. Workman, and J. Cote.** 2003. The diverse functions of histone acetyltransferase complexes. Trends Genet. **19:**321–329.
13. **Cartwright, R., A. M. Dunn, P. J. Simpson, C. E. Tambini, and J. Thacker.** 1998. Isolation of novel human and mouse genes of the recA/RAD51 recombination-repair gene family. Nucleic Acids Res. **26:**1653–1659.
14. **Dang, W., K. K. Steffen, R. Perry, J. A. Dorsey, F. B. Johnson, A. Shilatifard, M. Kaeberlein, B. K. Kennedy, and S. L. Berger.** 2009. Histone H4 lysine 16 acetylation regulates cellular lifespan. Nature **459:**802–807.
15. **Das, C., M. S. Lucia, K. C. Hansen, and J. K. Tyler.** 2009. CBP/p300-mediated acetylation of histone H3 on lysine 56. Nature **459:**113–117.
16. **Dion, M. F., S. J. Altschuler, L. F. Wu, and O. J. Rando.** 2005. Genomic characterization reveals a simple histone H4 acetylation code. Proc. Natl. Acad. Sci. U. S. A. **102:**5501–5506.
17. **Downs, J. A., S. Allard, O. Jobin-Robitaille, A. Javaheri, A. Auger, N. Bouchard, S. J. Kron, S. P. Jackson, and J. Cote.** 2004. Binding of chromatin-modifying activities to phosphorylated histone H2A at DNA damage sites. Mol. Cell **16:**979–990.
18. **Doyon, Y., W. Selleck, W. S. Lane, S. Tan, and J. Cote.** 2004. Structural and functional conservation of the NuA4 histone acetyltransferase complex from yeast to humans. Mol. Cell. Biol. **24:**1884–1896.
19. **Elledge, S. J.** 1996. Cell cycle checkpoints: preventing an identity crisis. Science **274:**1664–1672.
20. **Fernandez-Capetillo, O., S. K. Mahadevaiah, A. Celeste, P. J. Romanienko, R. D. Camerini-Otero, W. M. Bonner, K. Manova, P. Burgoyne, and A. Nussenzweig.** 2003. H2AX is required for chromatin remodeling and inactivation of sex chromosomes in male mouse meiosis. Dev. Cell **4:**497–508.
21. **Flicek, P., B. L. Aken, K. Beal, B. Ballester, M. Caccamo, Y. Chen, L. Clarke, G. Coates, F. Cunningham, T. Cutts, T. Down, S. C. Dyer, T. Eyre, S. Fitzgerald, J. Fernandez-Banet, S. Graf, S. Haider, M. Hammond, R. Holland, K. L. Howe, K. Howe, N. Johnson, A. Jenkinson, A. Kahari, D. Keefe, F. Kokocinski, E. Kulesha, D. Lawson, I. Longden, K. Megy, P. Meidl, B. Overduin, A. Parker, B. Pritchard, A. Prlic, S. Rice, D. Rios, M. Schuster, I. Sealy, G. Slater, D. Smedley, G. Spudich, S. Trevanion, A. J. Vilella, J. Vogel, S. White, M. Wood, E. Birney, T. Cox, V. Curwen, R. Durbin, X. M. Fernandez-Suarez, J. Herrero, T. J. Hubbard, A. Kasprzyk, G. Proctor, J. Smith, A. Ureta-Vidal, and S. Searle.** 2008. Ensembl 2008. Nucleic Acids Res. **36:**D707–D714.
22. **Gelbart, M. E., E. Larschan, S. Peng, P. J. Park, and M. I. Kuroda.** 2009. Drosophila MSL complex globally acetylates H4K16 on the male X chromosome for dosage compensation. Nat. Struct. Mol. Biol. **16:**825–832.
23. **Gentleman, R. C., V. J. Carey, D. M. Bates, B. Bolstad, M. Dettling, S. Dudoit, B. Ellis, L. Gautier, Y. Ge, J. Gentry, K. Hornik, T. Hothorn, W. Huber, S. Iacus, R. Irizarry, F. Leisch, C. Li, M. Maechler, A. J. Rossini, G. Sawitzki, C. Smith, G. Smyth, L. Tierney, J. Y. Yang, and J. Zhang.** 2004. Bioconductor: open software development for computational biology and bioinformatics. Genome Biol. **5:**R80.
24. **Gupta, A., T. G. Guerin-Peyrou, G. G. Sharma, C. Park, M. Agarwal, R. K. Ganju, S. Pandita, K. Choi, S. Sukumar, R. K. Pandita, T. Ludwig, and T. K. Pandita.** 2008. The mammalian ortholog of Drosophila MOF that acetylates histone H4 lysine 16 is essential for embryogenesis and oncogenesis. Mol. Cell. Biol. **28:**397–409.
25. **Gupta, A., G. G. Sharma, C. S. Young, M. Agarwal, E. R. Smith, T. T. Paull, J. C. Lucchesi, K. K. Khanna, T. Ludwig, and T. K. Pandita.** 2005. Involvement of human MOF in ATM function. Mol. Cell. Biol. **25:**5292–5305.
26. **Gupta, A., Q. Yang, R. K. Pandita, C. R. Hunt, T. Xiang, S. Misri, S. Zeng, J. Pagan, J. Jeffery, J. Puc, R. Kumar, Z. Feng, S. N. Powell, A. Bhat, T. Yaguchi, R. Wadhwa, S. C. Kaul, R. Parsons, K. K. Khanna, and T. K. Pandita.** 2009. Cell cycle checkpoint defects contribute to genomic instability in PTEN deficient cells independent of DNA DSB repair. Cell Cycle **8:**2198–2210.
27. **Haber, J. E.** 2000. Partners and pathways repairing a double-strand break. Trends Genet. **16:**259–264.
28. **Hunt, C. R., R. K. Pandita, A. Laszlo, R. Higashikubo, M. Agarwal, T. Kitamura, A. Gupta, N. Rief, N. Horikoshi, R. Baskaran, J. H. Lee, M. Lobrich, T. T. Paull, J. L. Roti Roti, and T. K. Pandita.** 2007. Hyperthermia activates a subset of ataxia-telangiectasia mutated effectors independent of DNA strand breaks and heat shock protein 70 status. Cancer Res. **67:**3010–3017.
29. **Huyen, Y., O. Zgheib, R. A. Ditullio, Jr., V. G. Gorgoulis, P. Zacharatos, T. J. Petty, E. A. Sheston, H. S. Mellert, E. S. Stavridi, and T. D. Halazonetis.** 2004. Methylated lysine 79 of histone H3 targets 53BP1 to DNA double-strand breaks. Nature **432:**406–411.
30. **Ikura, T., and V. V. Ogryzko.** 2003. Chromatin dynamics and DNA repair. Front. Biosci. **8:**s149–s155.
31. **Jeggo, P. A.** 1998. DNA breakage and repair. Adv. Genet. **38:**185–218.
32. **Kapoor-Vazirani, P., J. D. Kagey, D. R. Powell, and P. M. Vertino.** 2008. Role of hMOF-dependent histone H4 lysine 16 acetylation in the maintenance of TMS1/ASC gene activity. Cancer Res. **68:**6810–6821.
33. **Keeney, S.** 2001. Mechanism and control of meiotic recombination initiation. Curr. Top. Dev. Biol. **52:**1–53.
34. **Klipper-Aurbach, Y., M. Wasserman, N. Braunspiegel-Weintrob, D. Borstein, S. Peleg, S. Assa, M. Karp, Y. Benjamini, Y. Hochberg, and Z. Laron.** 1995. Mathematical formulae for the prediction of the residual beta cell

function during the first two years of disease in children and adolescents with insulin-dependent diabetes mellitus. Med. Hypotheses **45:**486–490.
35. **Kouzarides, T.** 2000. Acetylation: a regulatory modification to rival phosphorylation? EMBO J. **19:**1176–1179.
36. **Kurdistani, S. K., and M. Grunstein.** 2003. Histone acetylation and deacetylation in yeast. Nat. Rev. Mol. Cell Biol. **4:**276–284.
37. **Kurdistani, S. K., S. Tavazoie, and M. Grunstein.** 2004. Mapping global histone acetylation patterns to gene expression. Cell **117:**721–733.
38. **Kusch, T., L. Florens, W. H. Macdonald, S. K. Swanson, R. L. Glaser, J. R. Yates III, S. M. Abmayr, M. P. Washburn, and J. L. Workman.** 2004. Acetylation by Tip60 is required for selective histone variant exchange at DNA lesions. Science **306:**2084–2087.
39. **Li, X., L. Wu, C. A. Corsa, S. Kunkel, and Y. Dou.** 2009. Two mammalian MOF complexes regulate transcription activation by distinct mechanisms. Mol. Cell **36:**290–301.
40. **Lou, Z., K. Minter-Dykhouse, X. Wu, and J. Chen.** 2003. MDC1 is coupled to activated CHK2 in mammalian DNA damage response pathways. Nature **421:**957–961.
41. **Mahadevaiah, S. K., J. M. Turner, F. Baudat, E. P. Rogakou, P. de Boer, J. Blanco-Rodriguez, M. Jasin, S. Keeney, W. M. Bonner, and P. S. Burgoyne.** 2001. Recombinational DNA double-strand breaks in mice precede synapsis. Nat. Genet. **27:**271–276.
42. **Mendjan, S., M. Taipale, J. Kind, H. Holz, P. Gebhardt, M. Schelder, M. Vermeulen, A. Buscaino, K. Duncan, J. Mueller, M. Wilm, H. G. Stunnenberg, H. Saumweber, and A. Akhtar.** 2006. Nuclear pore components are involved in the transcriptional regulation of dosage compensation in Drosophila. Mol. Cell **21:**811–823.
43. **Misri, S., S. Pandita, R. Kumar, and T. K. Pandita.** 2008. Telomeres, histone code, and DNA damage response. Cytogenet. Genome Res. **122:**297–307.
44. **Morrison, A. J., J. Highland, N. J. Krogan, A. Arbel-Eden, J. F. Greenblatt, J. E. Haber, and X. Shen.** 2004. INO80 and gamma-H2AX interaction links ATP-dependent chromatin remodeling to DNA damage repair. Cell **119:** 767–775.
45. **Murr, R., J. I. Loizou, Y. G. Yang, C. Cuenin, H. Li, Z. Q. Wang, and Z. Herceg.** 2006. Histone acetylation by Trrap-Tip60 modulates loading of repair proteins and repair of DNA double-strand breaks. Nat. Cell Biol. **8:**91–99.
46. **Neal, K. C., A. Pannuti, E. R. Smith, and J. C. Lucchesi.** 2000. A new human member of the MYST family of histone acetyl transferases with high sequence similarity to Drosophila MOF. Biochim. Biophys. Acta **1490:**170–174.
47. **Ohba, R., D. J. Steger, J. E. Brownell, C. A. Mizzen, R. G. Cook, J. Cote, J. L. Workman, and C. D. Allis.** 1999. A novel H2A/H4 nucleosomal histone acetyltransferase in Tetrahymena thermophila. Mol. Cell. Biol. **19:**2061–2068.
48. **Pandita, R. K., G. G. Sharma, A. Laszlo, K. M. Hopkins, S. Davey, M. Chakhparonian, A. Gupta, R. J. Wellinger, J. Zhang, S. N. Powell, J. L. Roti Roti, H. B. Lieberman, and T. K. Pandita.** 2006. Mammalian Rad9 plays a role in telomere stability, S- and G2-phase-specific cell survival, and homologous recombinational repair. Mol. Cell. Biol. **26:**1850–1864.
49. **Pandita, T. K.** 1988. Assessment of the mutagenic potential of a fungicide Bavistin using multiple assays. Mutat. Res. **204:**627–643.
50. **Pandita, T. K.** 2002. ATM function and telomere stability. Oncogene **21:** 611–618.
51. **Pandita, T. K.** 1983. Effect of temperature variation on sister chromatid exchange frequency in cultured human lymphocytes. Hum. Genet. **63:**189–190.
52. **Pandita, T. K.** 2003. A multifaceted role for ATM in genome maintenance. Expert Rev. Mol. Med. **5**(16):1–21.
53. **Pandita, T. K.** 2001. The role of ATM in telomere structure and function. Radiat. Res. **156:**642–647.
54. **Pandita, T. K.** 2006. Role of mammalian Rad9 in genomic stability and ionizing radiation response. Cell Cycle **5:**1289–1291.
55. **Pandita, T. K., and W. N. Hittelman.** 1992. The contribution of DNA and chromosome repair deficiencies to the radiosensitivity of ataxia-telangiectasia. Radiat. Res. **131:**214–223.
56. **Pandita, T. K., and W. N. Hittelman.** 1992. Initial chromosome damage but not DNA damage is greater in ataxia telangiectasia cells. Radiat. Res. **130:** 94–103.
57. **Pandita, T. K., S. Pathak, and C. R. Geard.** 1995. Chromosome end associations, telomeres and telomerase activity in ataxia telangiectasia cells. Cytogenet. Cell Genet. **71:**86–93.
58. **Pandita, T. K., and C. Richardson.** 2009. Chromatin remodeling finds its place in the DNA double-strand break response. Nucleic Acids Res. **37:** 1363–1377.
59. **Pandita, T. K., C. H. Westphal, M. Anger, S. G. Sawant, C. R. Geard, R. K. Pandita, and H. Scherthan.** 1999. Atm inactivation results in aberrant telomere clustering during meiotic prophase. Mol. Cell. Biol. **19:**5096–5105.
60. **Peng, G., E. K. Yim, H. Dai, A. P. Jackson, I. Burgt, M. R. Pan, R. Hu, K. Li, and S. Y. Lin.** 2009. BRIT1/MCPH1 links chromatin remodelling to DNA damage response. Nat. Cell Biol. **11:**865–872.
61. **Pierce, A. J., R. D. Johnson, L. H. Thompson, and M. Jasin.** 1999. XRCC3 promotes homology-directed repair of DNA damage in mammalian cells. Genes Dev. **13:**2633–2638.
62. **Richard, D. J., E. Bolderson, L. Cubeddu, R. I. Wadsworth, K. Savage, G. G. Sharma, M. L. Nicolette, S. Tsvetanov, M. J. McIlwraith, R. K. Pandita, S. Takeda, R. T. Hay, J. Gautier, S. C. West, T. T. Paull, T. K. Pandita, M. F. White, and K. K. Khanna.** 2008. Single-stranded DNA-binding protein hSSB1 is critical for genomic stability. Nature **453:**677–681.
63. **Richardson, C., N. Horikoshi, and T. K. Pandita.** 2004. The role of the DNA double-strand break response network in meiosis. DNA Repair (Amst). **3:**1149–1164.
64. **Rodrigue, A., M. Lafrance, M. C. Gauthier, D. McDonald, M. Hendzel, S. C. West, M. Jasin, and J. Y. Masson.** 2006. Interplay between human DNA repair proteins at a unique double-strand break in vivo. EMBO J. **25:**222–231.
65. **Rothkamm, K., I. Kruger, L. H. Thompson, and M. Lobrich.** 2003. Pathways of DNA double-strand break repair during the mammalian cell cycle. Mol. Cell. Biol. **23:**5706–5715.
66. **Sanders, S. L., M. Portoso, J. Mata, J. Bahler, R. C. Allshire, and T. Kouzarides.** 2004. Methylation of histone H4 lysine 20 controls recruitment of Crb2 to sites of DNA damage. Cell **119:**603–614.
67. **Scherthan, H., M. Jerratsch, S. Dhar, Y. A. Wang, S. P. Goff, and T. K. Pandita.** 2000. Meiotic telomere distribution and Sertoli cell nuclear architecture are altered in Atm- and Atm-p53-deficient mice. Mol. Cell. Biol. **20:**7773–7783.
68. **Scott, S. P., and T. K. Pandita.** 2006. The cellular control of DNA double-strand breaks. J. Cell Biochem. **99:**1463–1475.
69. **Sharma, G. G., A. Gupta, H. Wang, H. Scherthan, S. Dhar, V. Gandhi, G. Iliakis, J. W. Shay, C. S. Young, and T. K. Pandita.** 2003. hTERT associates with human telomeres and enhances genomic stability and DNA repair. Oncogene **22:**131–146.
70. **Sharma, G. G., E. J. Hall, S. Dhar, A. Gupta, P. H. Rao, and T. K. Pandita.** 2003. Telomere stability correlates with longevity of human beings exposed to ionizing radiations. Oncol. Rep. **10:**1733–1736.
71. **Sharma, G. G., K. K. Hwang, R. K. Pandita, A. Gupta, S. Dhar, J. Parenteau, M. Agarwal, H. J. Worman, R. J. Wellinger, and T. K. Pandita.** 2003. Human heterochromatin protein 1 isoforms HP1(Hsalpha) and HP1(Hsbeta) interfere with hTERT-telomere interactions and correlate with changes in cell growth and response to ionizing radiation. Mol. Cell. Biol. **23:**8363–8376.
72. **Shia, W. J., B. Li, and J. L. Workman.** 2006. SAS-mediated acetylation of histone H4 Lys 16 is required for H2A.Z incorporation at subtelomeric regions in Saccharomyces cerevisiae. Genes Dev. **20:**2507–2512.
73. **Shia, W. J., S. G. Pattenden, and J. L. Workman.** 2006. Histone H4 lysine 16 acetylation breaks the genome's silence. Genome Biol. **7:**217.
74. **Shogren-Knaak, M., H. Ishii, J. M. Sun, M. J. Pazin, J. R. Davie, and C. L. Peterson.** 2006. Histone H4-K16 acetylation controls chromatin structure and protein interactions. Science **311:**844–847.
75. **Smith, E. R., C. Cayrou, R. Huang, W. S. Lane, J. Cote, and J. C. Lucchesi.** 2005. A human protein complex homologous to the Drosophila MSL complex is responsible for the majority of histone H4 acetylation at lysine 16. Mol. Cell. Biol. **25:**9175–9188.
76. **Sonoda, E., H. Hochegger, A. Saberi, Y. Taniguchi, and S. Takeda.** 2006. Differential usage of non-homologous end-joining and homologous recombination in double strand break repair. DNA Repair (Amst.). **5:**1021–1029.
77. **Soutoglou, E., J. F. Dorn, K. Sengupta, M. Jasin, A. Nussenzweig, T. Ried, G. Danuser, and T. Misteli.** 2007. Positional stability of single double-strand breaks in mammalian cells. Nat. Cell Biol. **9:**675–682.
78. **Sun, Y., X. Jiang, S. Chen, N. Fernandes, and B. D. Price.** 2005. A role for the Tip60 histone acetyltransferase in the acetylation and activation of ATM. Proc. Natl. Acad. Sci. U. S. A. **102:**13182–13187.
79. **Taipale, M., S. Rea, K. Richter, A. Vilar, P. Lichter, A. Imhof, and A. Akhtar.** 2005. hMOF histone acetyltransferase is required for histone H4 lysine 16 acetylation in mammalian cells. Mol. Cell. Biol. **25:**6798–6810.
80. **Tjeertes, J. V., K. M. Miller, and S. P. Jackson.** 2009. Screen for DNA-damage-responsive histone modifications identifies H3K9Ac and H3K56Ac in human cells. EMBO J. **28:**1878–1889.
81. **Tomimatsu, N., B. Mukherjee, and S. Burma.** 2009. Distinct roles of ATR and DNA-PKcs in triggering DNA damage responses in ATM-deficient cells. EMBO Rep. **10:**629–635.
82. **Tse, C., T. Sera, A. P. Wolffe, and J. C. Hansen.** 1998. Disruption of higher-order folding by core histone acetylation dramatically enhances transcription of nucleosomal arrays by RNA polymerase III. Mol. Cell. Biol. **18:**4629–4638.
83. **Turner, B. M., A. J. Birley, and J. Lavender.** 1992. Histone H4 isoforms acetylated at specific lysine residues define individual chromosomes and chromatin domains in Drosophila polytene nuclei. Cell **69:**375–384.
84. **Turner, B. M., L. P. O'Neill, and I. M. Allan.** 1989. Histone H4 acetylation in human cells. Frequency of acetylation at different sites defined by immunolabeling with site-specific antibodies. FEBS Lett. **253:**141–145.
85. **Vafa, O., M. Wade, S. Kern, M. Beeche, T. K. Pandita, G. M. Hampton, and G. M. Wahl.** 2002. c-Myc can induce DNA damage, increase reactive oxygen species, and mitigate p53 function: a mechanism for oncogene-induced genetic instability. Mol. Cell **9:**1031–1044.

86. **van Attikum, H., O. Fritsch, B. Hohn, and S. M. Gasser.** 2004. Recruitment of the INO80 complex by H2A phosphorylation links ATP-dependent chromatin remodeling with DNA double-strand break repair. Cell **119:**777–788.
87. **van Attikum, H., and S. M. Gasser.** 2009. Crosstalk between histone modifications during the DNA damage response. Trends Cell Biol. **19:**207–217.
88. **van Attikum, H., and S. M. Gasser.** 2005. The histone code at DNA breaks: a guide to repair? Nat. Rev. Mol. Cell Biol. **6:**757–765.
89. **Vaquero, A., A. Loyola, and D. Reinberg.** 2003. The constantly changing face of chromatin. Sci. Aging Knowledge Environ. **2003:**RE4.
90. **Vaquero, A., M. B. Scher, D. H. Lee, A. Sutton, H. L. Cheng, F. W. Alt, L. Serrano, R. Sternglanz, and D. Reinberg.** 2006. SirT2 is a histone deacetylase with preference for histone H4 Lys 16 during mitosis. Genes Dev. **20:**1256–1261.
91. **Vaquero, A., R. Sternglanz, and D. Reinberg.** 2007. NAD+-dependent deacetylation of H4 lysine 16 by class III HDACs. Oncogene **26:**5505–5520.
92. **Wu, Y., P. de Kievit, L. Vahlkamp, D. Pijnenburg, M. Smit, M. Dankers, D. Melchers, M. Stax, P. J. Boender, C. Ingham, N. Bastiaensen, R. de Wijn, D. van Alewijk, H. van Damme, A. K. Raap, A. B. Chan, and R. van Beuningen.** 2004. Quantitative assessment of a novel flow-through porous microarray for the rapid analysis of gene expression profiles. Nucleic Acids Res. **32:**e123.
93. **Wysocka, J., T. Swigut, T. A. Milne, Y. Dou, X. Zhang, A. L. Burlingame, R. G. Roeder, A. H. Brivanlou, and C. D. Allis.** 2005. WDR5 associates with histone H3 methylated at K4 and is essential for H3 K4 methylation and vertebrate development. Cell **121:**859–872.
94. **Zippo, A., R. Serafini, M. Rocchigiani, S. Pennacchini, A. Krepelova, and S. Oliviero.** 2009. Histone crosstalk between H3S10ph and H4K16ac generates a histone code that mediates transcription elongation. Cell **138:**1122–1136.